Leaf density and chemical composition explain variation in leaf mass area with spectral composition among 11 widespread forbs in a common garden

Wang, Qing-Wei

2021-11

Wang , Q-W , Liu , C , Robson , T M , Hikosaka , K & Kurokawa , H 2021 , ' Leaf density and chemical composition explain variation in leaf mass area with spectral composition among 11 widespread forbs in a common garden ' , Physiologia Plantarum , vol. 173 , no. 3 , pp. 698-708 . https://doi.org/10.1111/ppl.13512

http://hdl.handle.net/10138/346430
https://doi.org/10.1111/ppl.13512

acceptedVersion

Wang Qing-Wei (Orcid ID: 0000-0002-5169-9881)
Robson Thomas Matthew (Orcid ID: 0000-0002-8631-796X)

Leaf density and chemical composition explain variation in leaf mass area with spectral composition among 11 widespread forbs in a common garden

Qing-Wei Wang[1,2*], Chenggang Liu[3,4], Thomas Matthew Robson[5], Kouki Hikosaka[6], Hiroko Kurokawa[2]

[1]CAS Key Laboratory of Forest Ecology and Management, Institute of Applied Ecology, Chinese Academy of Sciences, Shenyang 110016, China

[2]Forestry and Forest Products Research Institute, 1 Matsunosato, Tsukuba, Ibaraki 3058687, Japan

[3]CAS Key Laboratory of Tropical Plant Resources and Sustainable Use, Xishuangbanna Tropical Botanical Garden, Chinese Academy of Sciences, Menglun 666303, China

[4]Center for Plant Ecology, Core Botanical Gardens, Chinese Academy of Sciences, Xishuangbanna 666303, China

[5]Organismal and Evolutionary Biology, Viikki Plant Science Centre (ViPS), P.O. Box 65, University of Helsinki, Helsinki 00014, Finland

[6]Graduate School of Life Sciences, Tohoku University, Sendai, Japan

***Corresponding Author information**

Qing-Wei Wang (wangqingwei@iae.ac.cn; wangqw08@gmail.com; Tel: +86-(0)24-8397-0329)

Abstract

Leaf mass per area (LMA) is a key leaf functional trait correlated with plant strategies dictating morphology, physiology, and biochemistry. Although sunlight is generally accepted as a dominant factor driving LMA, the contribution of each spectral region of sunlight in shaping LMA is poorly understood. In the present study, we grew 11 widespread forb species in a common garden and dissected the traits underpinning differences in LMA, such as its morphological components (leaf density (LD), and leaf thickness (LT)), macroelement and metabolite composition under five spectral-attenuation treatments: (1) transmitting c. 95% of the whole solar spectrum (> 280 nm), (2) attenuating ultraviolet-B radiation (UV-B), (3) attenuating both UV-A and UV-B radiation, (4) attenuating UV radiation and blue light, (5) attenuating UV radiation, blue, and green light. We found that LMA, LD, and chemical traits varied significantly across species depending on spectral treatments. LMA was significantly

This article has been accepted for publication and undergone full peer review but has not been through the copyediting, typesetting, pagination and proofreading process which may lead to differences between this version and the Version of Record. Please cite this article as doi: 10.1111/ppl.13512

increased by UV-B radiation and green light, while LD was increased by UV-A but decreased by blue light. LMA positively correlated with LD across treatments but was only weakly related to LT, suggesting that LD was a better determinate of LMA for this specific treatment. Regarding leaf elemental and metabolite composition, carbon, nitrogen, and total phenolics were all positively correlated with LMA, whereas lignin, non-structural carbohydrates, and soluble sugars had negative relationships with LMA. These trends imply a tradeoff between biomass allocation to structural and metabolically functional components. In conclusion, sunlight can spectrally drive LMA mainly through modifying functional and structural support.

Keywords: functional traits, leaf mass per area, plasticity, spectral regions, ultraviolet radiation.

1-Introduction

Plant functional traits generally reflect trade-offs in plant acquisition/investment according to the limiting resources in their environments (Wright et al. 2004). Leaf mass per area (LMA), as the key trait to the 'leaf economic spectrum (LES)', is an indicator of leaf physiological and morphological function (e.g. photosynthesis and defense) (Reich et al. 1997, Poorter et al. 2009, Poorter et al. 2019), as well as ecosystem properties and processes (e.g. primary productivity and litter decomposability) (Wright et al. 2004, Cornwell et al. 2008, Adler et al. 2014, Duursma and Falster 2016). A better understanding of the abiotic drivers (e.g. light) of variations in LMA, and the structural and compositional basis of LMA, is required to improve our capacity to predict how ecosystem functioning responds to ongoing climate changes (e.g. cloudiness, aerosol pollutants, and forest fires).

LMA is determined by two structural components, leaf thickness (LT) and leaf density (LD, dry mass per unit volume): LMA = LT × LD (Witkowski and Lamont 1991b, Poorter et al. 2009). Increases in LT are primarily associated with additional mesophyll thickness (e.g. increase in the layers and volumetric fraction of palisade cells) (Niinemets 1999, Griffith et al. 2016, Coble and Cavaleri 2017). A higher LT can contribute to higher photosynthetic capacity under high light (Oguchi et al. 2005) or higher water use efficiency under drought conditions (Wright et al. 2002). Variation in LD is generally related to changes in mesophyll cell size, air spaces, and the volume fraction of the cell wall (Niinemets 1999, Poorter et al. 2009). Tightly packed mesophyll cells with thickened cell walls would increase LD and constrain mesophyll conductance, limiting photosynthesis and carbon (C) uptake (Niinemets 2001, John et al. 2017), but increase robustness against water loss and herbivory (Peeters 2002). On the other hand, leaf nutrients or chemical compounds per unit leaf area are positively related to LD and LMA

(Poorter and Villar 1997, Poorter et al. 2009). For instance, LMA increases with a greater proportion of leaf C (de la Riva et al. 2016) and total non-structural carbohydrates (NSC) (Xu et al. 2012), and with low nitrogen (N) concentration (de la Riva et al. 2018). Therefore, the extent to which LMA responds to environmental changes strongly depends on its structural and functional basis.

A large number of studies focusing on the plasticity of LMA to abiotic factors have found that it responds to numerous changes in environmental conditions in nature; the factors driving variation in LMA include light (Coble and Cavaleri 2015, Fajardo and Siefert 2016), temperature (Fajardo and Piper 2011, Zhang et al. 2020), water (Sanchez-Gomez et al. 2013, Fernandez-Martinez et al. 2016), nutrients (Onoda et al. 2008, Wang et al. 2019), and CO_2 (Ishizaki et al. 2003, Hikosaka et al. 2005). However, a meta-analysis from Poorter et al. (2009) has identified that light is the dominant factor driving LMA variation, exceeding temperature in importance, based on LMA data from a total of 3800 species across functional groups and ecosystems types. The positive correlation across species between irradiance and LMA suggests that plants may have strategically adapted to changes in light conditions to increase leaf area for light interception under low light and photosynthetic capacity under high light. Poorter et al. (2019) further generalized irradiance–response curves for 70 traits related to leaf morphology, chemistry, and physiology of 760 species: Plasticity in both LT and LD tended to double over the studied light range (0.2-75 mol m^{-2} d^{-1}), equally contributing to the 2.6-fold increase in LMA from low to high irradiance. Although previous meta-analyses provide a general picture of the response to light intensity (quantity), the related mechanisms behind these responses, particularly the extent to which such changes are determined by spectral composition, are less well described.

Sunlight does not only supply the essential energy input for photosynthesis (Moss 1967, Hikosaka et al. 1994, Oguchi et al. 2017), but importantly provides cues that regulate leaf traits and dictate plant functional strategy (Jenkins et al. 2001, Ballaré 2014, Wang et al. 2020). The incident solar radiation is composed of multiple spectral regions, which are important for plant function, from ultraviolet (UV)-B (280–315 nm) to red light (600–700 nm). Photoreceptors absorb specific spectral regions and are well documented to regulate a set of molecular, physiological, and biochemical processes (Smith et al. 2017, Verdaguer et al. 2017, Casal and Qüesta 2018, Robson et al. 2019). Briefly, UV-B radiation (280–315 nm) and UV-A radiation below 350 nm sensed by UVR8 (UV RESISTANCE LOCUS8) can induce the synthesis of UV-absorbing compounds (e.g. phenolics) to attenuate excess UV-B radiation (Casati et al. 2011, Rai et al. 2019). Blue light (400-500 nm) increases LMA and leaf N concentration, and

promotes photosynthetic efficiency (Hogewoning et al. 2010) through activating photoreceptors, cryptochromes (CRYs), phototropins (PHOTs) and proteins from the zeitlupe family (Casal 2000, Lin 2000). Red light (600-700 nm) decreases LMA, LT, N and NSC concentrations (Hu et al. 2016, Liu et al. 2018) by activating phytochromes (PHYs) (Smith 2000). Green light (500-600 nm) induces shading syndromes antagonistically to blue light (Smith et al. 2017). However, even though the roles of each spectral region have been explored in molecular biology and actively applied in horticulture (Hogewoning et al. 2010, Brelsford et al. 2019, O'Hara et al. 2019, Rai et al. 2019), the ecophysiology behind how these regions of sunlight interact to affect plant functional traits outdoors has not been entirely resolved, since multiple wavebands may coordinate leaf responses simultaneously through crosstalk among photoreceptors (Casal 2000, Rai et al. 2019).

Although several ecological studies have focused on responses to changing UV-B radiation and red to far-red ratio (R/Fr) to respectively assess how plants acclimate to UV-B stress (Searles et al. 2001, Rousseaux et al. 2004) and shade (Aphalo and Lehto 2001, Razzak et al. 2017), spectral regions from the photosynthetically active radiation (PAR) are not often included in such studies. In the present study, we assessed variation in LMA and components (both morphological and chemical) of 11 common forb species growing under spectral-attenuation-filter treatments. We aimed to answer the questions: (1) Which spectral regions determine LMA? (2) How does variation in LD and LT explain changes in LMA? (3) Is the change in LMA with spectral composition related to differences in leaf metabolic, structure and elemental composition?

2-Materials and methods

2.1 Plant materials

The present study used 11 widespread light-demanding forb species (see species list in Table 1). Most species are sun plants, but some favours shade conditions. Seeds were collected from Tsukuba Botanical Garden, National Museum of Nature and Science, Tsukuba, Japan (36°00′N, 140°08′E). Seeds were sown on 25th May 2018 into pots with a volume of 438 cm^3 (9.0 × 7.6 × 6.4 cm) in a greenhouse of the Forestry and Forest Products Research Institute (FFPRI), Tsukuba, after vernalization on wet filter papers for 4 days at 4°C in the dark. The order of sowing seeds was opposite to the germination order, and the timing was controlled to ensure the initial age of seedlings was relatively homogenous across species. Pots were filled with a mixture of compost, including vermiculite, kanuma soil, and pumice [6:1:2:1(v/v)]. We watered pots from beneath through the trays every 3 days and supplied nutrients once per week

with a commercial liquid fertilizer (N–P–K = 6–10–5%, HYPONEX, Japan). The nutrient dose was diluted to a concentration of 1.2 mL/L, 7.5 mL/pot. Dead individuals during the experimental period were removed.

2.2 Experimental growth conditions

We carried out this spectral-attenuation experiment in a large unshaded garden at FFPRI. Details are described in a previous study (Wang et al. 2020). Briefly, we attached the plastic filters to 1.2 × 1.0 m wooden frames at around 20° inclination (facing south), with additional filter pieces on both the East and West sides of frames, in order to attenuate diffuse sunlight early and late in the day. Five spectral irradiance treatments included: (1) Full-spectrum treatment (transmitting λ >280 nm, i.e. all solar UV-B), with a fully transparent polythene film (0.05 mm thick, 3904CF; Okura), transmitting approximately 95% of the whole solar spectrum; (2) No-UVB treatment (λ >315 nm), attenuating UV-B radiation (0.125-mm-thick polyester film, Autostat CT5; Thermoplast); (3) No UV treatment (λ >400 nm), attenuating all UV radiation (0.2-mm-thick Rosco E-Color 226 filter, Westlighting); (4) No UV/Blue treatment (λ >500 nm), attenuating all UV and blue wavelengths (0.20-mm-thick Roscolux Supergel 312 filter); (5) No-UV and blue–green (UV/BG) treatment (λ >580 nm), attenuating all UV radiation and BG wavelengths (0.2-mm-thick Rosco E-Color 135 Deep Golden Amber filter) (Table 2).

Due to differences in transmittance ratios among filters, we added different types of spectrally neutral shade mesh below the filters, allowing seedlings to receive equivalent PAR irradiance across treatments. The average PAR under each frame was 14% of ambient sunlight (Table 2), determined by a quantum sensor (LI-190, Li-Cor Biosciences Inc). Attenuating solar radiation to create treatments at equivalent PAR irradiance allowed us to better distinguish spectral treatment effects rather than damage from high irradiance. The spectrum treatment created by each filter was determined under a clear sky at solar noon using a spectroradiometer (USR- 45DA; USHIO). The spectral irradiance under each frame during the experiment was checked using a Maya 2000 Pro array spectrometer (Ocean Optics Inc.) calibrated for maximum spectral sensitivity in solar UV and PAR (Hartikainen et al. 2018).

The whole experiment was arranged in four randomised blocks of filters (in total 20 filter-frames), each block being a replicate (Fig. S1). Twenty individuals of each species were randomly separated among the 20 filter-frames on 23rd June 2018. Plants were placed in two plastic trays (51 × 31 × 5.3 cm) on a wooden shelf under the center of each frame to limit the diffuse solar radiation from outside. We changed filter height to keep them suspended around

20-cm above the upper leaves, and randomly rotated the position of the pots every week to ensure all seedlings grew in similar light conditions throughout the experiment. We supplied water twice a day (once at 8:00 am and 7:00 pm for 60 s) using a purpose-built sprinkler system. Nutrients were supplied in the same way described above. Ambient PAR, UV-B, and UV-A radiation (Fig. S2A, B) were measured and integrated over 15-min intervals using the LI-190SA sensor and two broadband UV-cosine sensors (UV-B and UV-A; sglux GmbH), respectively, with a data-logger (LI-1400; LI-COR). Air temperature approximately 20 cm above the pots (Fig. S2C) was recorded at 30-min intervals using a HOBO H8 Pro temperature logger (Onset Computer Corporation, Bourne).

2.3 Measurements of leaf traits

Fully expanded sun leaves (2–4 leaves per individual) were collected for chemical analysis under a clear-sky sunny day (27th August 2018) at the end of the growing season. Leaf samples were ground into a fine powder after vacuum-drying (FDU–1200, EYELA) for 16 h. Leaf C and N concentrations were measured using an elemental analyser (Vario MAX cube). The concentration of total phenolics was determined by the Folin-Ciocalteu method using tannic acid as a standard sample (Waterman and Mole 1994). The concentration of lignin was measured by an improved acetyl-bromide procedure (Iiyama and Wallis 1990) and calculated from the fitted calibration curve (Fukushima and Hatfield 2001). The concentration of the condensed tannins was determined by a proanthocyanidin assay using cyanidin chloride as a standard sample (Julkunen-Tiitto 1985). The concentrations of total soluble sugars and starch were determined using the anthrone method (Wang et al. 2018b). We defined non-structural carbohydrates (NSC) as the sum of total soluble sugars and starch. All chemical traits were expressed on a dry-matter basis (% dm) and an area basis (g m^{-2}).

Another equivalent pair of leaves were collected for measuring leaf morphological traits on 28th August 2018. Leaf area (LA, cm^2) was scanned and calculated with the Fiji software (Wang et al. 2021). LT (μm) was measured in four random places with a thickness gauge (model 547-401m, 0.001mm; Mitutoyo), avoiding both primary and secondary veins. The measured leaves were dried in an oven at 60°C for 48 h to obtain leaf dry mass (LM, g). LMA (g m^{-2}) was determined based on LA and LM of scanned leaves. LD (g cm^{-3}) was calculated from LM divided by LT and LA. Sampling was not done for two dead species (*Adenophora triphylla* var. *japonica* and *Prunella vulgaris* L.) in the No-UVB treatment, and one in No-UV/BG treatment (*P. vulgaris* L.) during the experiment.

2.4 Statistical analyses

Linear mixed effect models (LME) were fitted for each leaf trait with spectral treatment as the fixed factor, and species and blocks as random factors, which reduced the effects of plant size and frame position, using the *nlme* package (Pinheiro and Bates 2000). When the treatment was significant ($P < 0.05$), further analysis assessed the effects of specific wavelength regions by pairwise contrasts (function *glht*, R package *multcomp*, Hothorn et al. 2008). The contrasts between the spectral treatments: >315 nm vs >280 nm, >400 nm vs >315 nm, >500 nm vs >400 nm, >580 nm vs >500 nm, estimate the effect of UV-B, UV-A, blue light, and green light, respectively. Benjamini-Hochberg (BH)'s method (Benjamini and Hochberg 1995) was used to correct *P*-values for multiple comparisons. Linear least squares method was used to analyse the correlations among leaf morphological and chemical traits. Extra sum-of-squares *F* test was used to test whether slopes and intercepts were significantly different. The Box–Cox transformation was applied where appropriate to ensure the normality of response variables (Yeo and Johnson 2000). In addition, the present experiment pre-included three shade-tolerant species. However, we found the robustness of the relationships between LMA and functional traits were very weak for shade-tolerant species. Finally, we removed this data and use those of shade-intolerant species only.

3-Results

3.1-Spectral-attenuation treatments lead to variation in leaf traits

In the experiment, we firstly measured the 13 leaf traits covering a wide range of variation across the 11 studied species (Table 1) and observed differences of between 1.2~9.6 times among species. Across all species in general, LMA and LD were significantly affected by our solar spectral-attenuation treatments (Fig. 1, S3, 4), despite receiving equivalent PAR and temperature (Fig. S2). Contrast comparisons found that LMA was significantly reduced by the attenuation of UV-B radiation (by 6.7%) and green light (by 5.9%) (Fig. 1A), whereas LD significantly decreased and increased when either UV-A radiation and blue light were attenuated, respectively (Fig. 1B).

In terms of chemical traits on a dry-mass basis, concentrations of C, N, and total phenolics were significantly reduced by the attenuation of blue light (Fig. S4A, B, C), while concentrations of C and total phenolics also decreased when green light and UV-B radiation were attenuated, respectively. Lignin concentration was significantly increased by the attenuation of UV-B radiation (Fig. S4D). Concentrations of tannins, NSCs, and total soluble

sugars were significantly reduced by the attenuation of green light (Fig. S4E, F, G), whereas total soluble sugars also increased when UV-B radiation was attenuated. Starch concentration significantly decreased with the attenuation of UV-A radiation (Fig. S4H). These traits on an area basis tended to decrease consistently from Full-spectrum to No-UV/BG treatment; concentrations of most macroelements and metabolites (all except for NSC and starch) were significantly reduced by the attenuation of green light (Fig. S5).

3.2-Relationships between leaf traits among spectral-attenuation treatments

LMA was positively correlated with LD across spectral treatments with similar slopes (R^2 = 0.48−0.62, P < 0.05, Table S1, Fig. 2A), but not with LT; except for one negative relationship from the No-UV treatment (R^2 = -0.48, P = 0.02, Fig. 2B). There were no significant relationships between either of the two components (LD and LT) of LMA, irrespective of spectral treatment (Fig. 2C).

LMA was positively correlated with the concentrations of C, N, and total phenolics on a dry-mass basis (R^2 = 0.09−0.31, P < 0.05, Table S1, Fig. 3A), but negatively correlated with the concentrations of lignin, NSCs, and total soluble sugars (R^2 = -0.20−-0.14, P < 0.05) across all treatments. Regarding each spectral treatment, LMA was positively related with C concentration in the Full-spectrum, No-UVB, and No-UV/BG treatments (R^2 = 0.46–0.66, P < 0.05), and with N concentration in the Full-spectrum, No-UV/Blue, and No-UV/BG treatments (R^2 = 0.36–0.69, P < 0.05).

As a whole, LD was also positively correlated with the concentration of total phenolics (R^2 = 0.08, P = 0.04, Table S1, Fig. 3B), and negatively with concentrations of lignin, NSCs, and total soluble sugars (R^2 = -0.09–-0.29, P < 0.05). Significant relationships of LD with NSCs and total soluble sugars at the treatment level were detected in the No-UVB and No-UV/BG treatments. However, there were no relationships of LD with C or N concentration (P > 0.05).

LT was negatively correlated with the concentrations of C, N, and tannin (R^2 = -0.30–-0.10, P < 0.05, Table S1, Fig. 3C) across all treatments. Specifically, LT had negative relationships with N concentration in the Full-spectrum, No-UVB, and No-UV treatments (R^2 = -0.53–-0.36, P < 0.05), and with tannins in the Full-spectrum and No-UVB treatments (R^2 = -0.53–-0.41, P < 0.05).

These relationships in each treatment were weak on an area basis (except for those with total soluble sugars, Table S2), whereas LMA and LT were generally positively correlated with C and N for the pooled data, and negatively with other metabolites and structural traits.

4-Discussion

4.1-Solar spectral regions determining LMA and its components

We found that LMA significantly decreased when UV-B radiation was attenuated (Fig.1A). Such a UV-B effect is congruent with most previous findings of irradiance dose-response studies because high global irradiance almost always coincided with high UV-B irradiance in the field. For instance, LMA is generally higher across scales of leaves and species that grow in "high light" environments, i.e. higher in shade-intolerant than shade-tolerant herb and woody species (Niinemets 1997, Zhang et al. 2019), and for leaves at the canopy top than those within the canopy (Coble and Cavaleri 2014, 2015). High UV-B irradiance not only promotes the accumulation of specific phenolic compounds in epidermal tissues (also see Fig. S4C) that act as UV-absorbing sunscreens (Åke et al. 1994), but also increases LMA to improve UV tolerance, i.e. through denser and more compact leaves (Berli et al. 2012). Recent mechanistic studies have revealed that these UV-B responses are regulated by photomorphogenesis mediated by UVR8 (Rizzini et al. 2011, Hayes et al. 2014, Jenkins 2017). However, a meta-analysis study has not detected a consistent response of LMA to high UV-B irradiance across species of different functional groups and ecosystem types (Poorter et al. 2009), probably due to insufficient data from controlled experiments rather than field monitoring, or maybe because so many ubiquitous environmental drivers (e.g. temperature and moisture) interact strongly with sunlight to shape LMA (Wang et al. 2018a).

Interestingly, in addition to indicators of "high light" like UV-B radiation, green light also significantly increased LMA in our experiment from the comparison between No-UV/Blue and No-UV/BG treatments (Fig.1A). Molecular and horticulture studies find that green light generally causes two distinct photomorphogenic effects. It can act as a 'shade' cue antagonistically to blue light, promoting a more shade-acclimated phenotype (Zhang et al. 2011, Smith et al. 2017). Green light can penetrate deeper into the mesophyll layer than blue and red light (Terashima et al. 2009) and contributes a significant proportion of photosynthetic C assimilation in deeper leaf tissues (Smith et al. 2017). This latter mechanism may explain the change in LMA under green light found in our study, which requires clarification through further specific studies.

Regarding the components of LMA, LD rather than LT significantly responded to our spectral treatments, each of which decreased and increased with the attenuation of UV-A and blue light, respectively (Fig. 1B, C). This trend implies that mass allocation or investment within the leaf is more plastic than leaf structure to the changes in spectral composition. Higher LD may reflect smaller cells with thicker cell walls (Garnier and Laurent 1994), lower volume

of airspaces (Coble and Cavaleri 2017), and a higher proportion of sclerified tissues (Niinemets 2001). Such 'sun-leaf type' characteristics may be mediated by UV-A radiation (Verdaguer et al. 2017), which is perceived by UVR8 (Casati et al. 2011, Rai et al. 2019) and CRYs (Casal 2013). Both photoreceptors can regulate light acclimation, e.g. through an increase in palisade cells and photoprotective pigments. However, it is not clear why blue light rather reduced LD in our experiment (Fig. 1B). One possible interpretation is that blue light generally stimulates an increase in stomatal conductance (Hogewoning et al. 2010, Terfa et al. 2013), which may also result in a high proportion of leaf internal air space, consequently contributing to a low LD.

4.2-Variation in LD explains changes in LMA in response to spectral composition

LMA positively correlated with LD across all spectral treatments (Fig. 2A), whereas it negatively correlated with LT only in the treatment where UV radiation was attenuated (Fig. 2B). These results suggest that the dependency of LMA on LD is consistent across multiple spectral compositions and inherent among our studied species. This conclusion agrees with previous findings, for example, that LD is a better driver of LMA than LT among 769 native herbs in the field (Wilson et al. 1999) and 14 grasses in the growth room (Garnier and Laurent 1994). However, all three metrics (LMA, LD, and LT) significantly increase with the rise in solar irradiance from the understorey to canopy top to the forest canopy (Coble and Cavaleri 2014, 2015, Zhang et al. 2019). These patterns imply that the dependency of LMA on LD may be determined by spectral composition (light quality), but that the strength of irradiance (light intensity) mediates how both LD and LT affect LMA.

This dissociation between the effects of the sunlight intensity and its composition is permitted by the independent relationship between LD and LT (Fig. 2C). Earlier studies have also found LD and LT to respond independently to environmental conditions (Niinemets 1999, Kitajima and Poorter 2010), with LT generally greater under stress conditions, such as high light, drought, and low temperature (Poorter et al. 2009, Poorter et al. 2019). Higher LT implies that a greater fraction of leaf tissues is allocated to the mesophyll (Sancho-Knapik et al. 2020), especially in palisade layer, which maximizes overall absorption (Coble and Cavaleri 2017). Thus, increased LT together with higher LD under strong irradiance would contribute to greater net C assimilation rate and shorten the "leaf pay-back time" (Niinemets 2001, Poorter et al. 2019). Under the low irradiance, however, high LMA and LD may be advantageous at the expense of short-term C gain (Kitajima 1994, Valladares and Niinemets 2008), since increased LD is associated with a decrease in assimilative compounds and modifications in leaf anatomy

(Niinemets 1999).

4.3-The relationship between leaf morphology and leaf chemical compositions

Based on relationships of LD and LT with leaf chemical compositions, we could understand the allocation strategy in structural components and metabolically functional components when plants receive different spectral compositions. LMA and leaf chemical composition covaried according to the spectral composition of growing conditions (Table S1). LMA was positively correlated with C and N concentration across multiple spectral treatments (Fig. 3A), confirming that higher LMA is related to a higher fraction of C in structural tissues (de la Riva et al. 2018) and of N in physiological functioning. Such results seem not support the trade-off in investment between mechanical support and physiological activity, according to the leaf economics spectrum theory (Wright et al. 2004). This expectation is based on the hypothesis that higher C and N allocation to cell walls results in higher mechanical resistance, while the decrease in N to photosynthetic proteins reduces photosynthesis (Onoda et al. 2017). However, the cell wall represents only one aspect of leaf mechanical properties, which also include e.g. cuticle, fibers, and veins (Onoda et al. 2011), while the fraction of N allocated to the cell wall and proteins also varies among species (Onoda et al. 2017). In other words, it is not a given that a higher cell wall fraction leads to less N allocated to photosynthetic apparatus. This possibility is supported by a study that found leaf mechanical strength to vary independently from photosynthetic capacity across 57 shade-tolerant and light-demanding species (He et al. 2019).

As a whole, LMA and LD were negatively correlated with mass-based concentrations of lignin, NSCs, and sugars (Fig. 3A, B). This relationship indicates a trade-off between LMA and metabolite accumulation per leaf mass, which may be the result of greater mass allocation to structural components than metabolically functional components (those contribute to improve stress tolerance) with a high LMA (Li et al. 2013). Notably, LMA and LD were positively correlated with mass-based concentrations of total phenolics (Fig. 3A, B), the dominant compounds of stress tolerance. Phenolics are C-rich compounds (ca. 30% C on a mass basis) compared with proteins (Poorter 1994), and their accumulation in leaf vacuoles and cell walls can increase LD (Witkowski and Lamont 1991a). In addition, these dependencies of LMA on metabolite composition were less differentiated among spectral treatments (Fig. 3A, Table S1), perhaps due to the overlapping action spectra of photoreceptors. It is known that the synthesis of specialized (secondary) metabolites is generally mediated by multiple wavelength regions (Casal 2013, Robson et al. 2015, Smith et al. 2017, Verdaguer et al. 2017,

Casal and Qüesta 2018). Their combined effects would be synergistic, additive or antagonistic when plants simultaneously receive light from multiple regions (Rai et al. 2019, Wang et al. 2020). Nevertheless, the relationships discussed above need to be confirmed in more species, since the present experiment just used 11 species, which may limit the robustness

5-Conclusions

The present study demonstrates that LMA and its morphological components, and leaf elemental and metabolite compositions varied significantly in response to solar spectral composition across 11 forb species in spectral attenuation treatments receiving the same PAR irradiance. LMA variation was determined by UV-B radiation and green light, and in general was mainly dependent on LD rather than LT. Changes in leaf elemental and metabolic composition, on the mass-basis, under our spectral attenuation treatments were associated with changes in LMA, which implies a trade-off in biomass allocation between structural and metabolically functional components. These results suggest that the spectral composition of solar radiation can regulate LMA irrespective of total irradiance by modifying mass investment and structural support.

Authors' contributions: Q.-W.W., H.K. and T.M.R. conceived and designed the experiment; Q.-W.W. carried out the growth experiment and performed most trait measurements; C.G.L. determined concentrations of leaf total soluble sugars and starch; Q.-W.W. provided statistical analysis; Q.-W.W. wrote the draft of the manuscript, and K.H., T.M.R., H.K, and C.G.L. revised the manuscript.

Acknowledgements

We thank Drs Qingmin Han and Jun Hidema for spectral equipment support, Dr Yoshinori Murai for seed collection, Drs Mitsue Shibata and Tamotsu Sato for facilities at FFPRI, and Nobuko Hirai, Masako Hosoi, Yasuko Ogane, Hiroko Shiomi, Rie Takaya for their help with laboratory work. Q.-W. Wang is grateful to the Japan Society for the Promotion of Science (JSPS), Japan for awarding the JSPS Post-doctoral Research Fellowship for Foreign Researchers in Japan (FY 2017-2019). This study was supported by KAKENHI (17F17403) to Q.-W.W. and H.K., and by KAKENHI (17H03736) to H.K. and by the CAS Young Talents Program, National Natural Science Foundation of China (NSFC) (41971148), and LiaoNing Revitalization Talents Program (XLYC2007016) to Q.-W.W., and by the CAS Youth Innovation Promotion Association (2019388) and the Yunnan Fundamental Research Projects

of China (2018FB042) to C.G.L. T.M.R. was supported by the Academy of Finland decisions #304519 and #324555.

Data availability statement

The data that support the findings of this study are available on request from the corresponding author.

References

Adler PB, Salguero-Gomez R, Compagnoni A, Hsu JS, Ray-Mukherjee J, Mbeau-Ache C, Franco M (2014) Functional traits explain variation in plant life history strategies. Proc Natl Acad Sci U S A 111(2): 740-745

Åke S, Wah Soon Chow, Anderson JM (1994) UV-B damage and protection at the molecular level in plants. Photosynth Res 39: 475-489

Aphalo PJ, Lehto T (2001) Effect of lateral far-red light supplementation on the growth and morphology of birch seedlings and its interaction with mineral nutrition. Trees-Struct Funct 15(5): 297-303

Ballaré CL (2014) Light regulation of plant defense. Annu Rev Plant Biol 65: 335-363

Benjamini Y, Hochberg Y (1995) Controlling the false discovery rate: a practical and powerful approach to multiple testing. Journal of the Royal Statistical Society Series B (Methodological) 57: 289-300

Berli FJ, Alonso R, Bressan-Smith R, Bottini R (2012) UV-B impairs growth and gas exchange in grapevines grown in high altitude. Physiol Plant 149(1): 127-140

Brelsford CC, Morales LO, Nezval J, Kotilainen TK, Hartikainen SM, Aphalo PJ, Robson TM (2019) Do UV-A radiation and blue light during growth prime leaves to cope with acute high light in photoreceptor mutants of Arabidopsis thaliana? Physiol Plant 165(3): 537-554

Casal JJ (2000) Phytochromes, cryptochromes, phototropin: photoreceptor interactions in plants. Photochem Photobiol 71(1): 1-11

Casal JJ (2013) Photoreceptor signaling networks in plant responses to shade. The Annual Review of Plant Biology 64: 403-427

Casal JJ, Qüesta JI (2018) Light and temperature cues: multitasking receptors and transcriptional integrators. new phytologist 217(3): 1029-1034

Casati P, Campi M, Morrow DJ, Fernandes JF, Walbot V (2011) Transcriptomic, proteomic and metabolomic analysis of UV-B signaling in maize. BMC Genomics 12(1): 321

Coble AP, Cavaleri MA (2014) Light drives vertical gradients of leaf morphology in a sugar maple (Acer saccharum) forest. Tree Physiol 34(2): 146-158

Coble AP, Cavaleri MA (2015) Light acclimation optimizes leaf functional traits despite height-related constraints in a canopy shading experiment. Oecologia 177(4): 1131-1143

Coble AP, Cavaleri MA (2017) Vertical leaf mass per area gradient of mature sugar maple reflects both height-driven increases in vascular tissue and light-driven increases in palisade layer thickness. Tree Physiol 37(10): 1337-1351

Cornwell WK, Cornelissen JH, Amatangelo K, Dorrepaal E, Eviner VT, Godoy O, Hobbie SE, Hoorens B, Kurokawa H, Perez-Harguindeguy N, Quested HM, Santiago LS, Wardle DA, Wright IJ, Aerts R, Allison SD, van Bodegom P, Brovkin V, Chatain A, Callaghan TV, Diaz S, Garnier E, Gurvich DE, Kazakou E, Klein JA, Read J, Reich PB, Soudzilovskaia NA, Vaieretti MV, Westoby M (2008) Plant species traits are the predominant control on litter decomposition rates within biomes worldwide. Ecol Lett 11(10): 1065-1071

de la Riva EG, Olmo M, Poorter H, Ubera JL, Villar R (2016) Leaf mass per area (LMA) and its relationship with leaf structure and anatomy in 34 Mediterranean woody species along a water availability gradient. PLoS One 11(2): e0148788

de la Riva EG, Villar R, Perez-Ramos IM, Quero JL, Matias L, Poorter L, Maranon T (2018) Relationships between leaf mass per area and nutrient concentrations in 98 Mediterranean woody species are determined by phylogeny, habitat and leaf habit. Trees-Struct Funct 32(2): 497-510

Duursma RA, Falster DS (2016) Leaf mass per area, not total leaf area, drives differences in above-ground biomass distribution among woody plant functional types. New Phytologist 212(2): 368-376

Fajardo A, Piper FI (2011) Intraspecific trait variation and covariation in a widespread tree species (Nothofagus pumilio) in southern Chile. New Phytologist 189(1): 259-271

Fajardo A, Siefert A (2016) Temperate rain forest species partition fine-scale gradients in light availability based on their leaf mass per area (LMA). Ann Bot 118(7): 1307-1315

Fernandez-Martinez J, Fransi MA, Fleck I (2016) Ecophysiological responses of Betula pendula, Pinus uncinata and Rhododendron ferrugineum in the Catalan Pyrenees to low summer rainfall. Tree Physiol 36(12): 1520-1535

Fukushima RS, Hatfield RD (2001) Extraction and isolation of lignin for utilization as a standard to determine lignin concentration using the acetyl bromide spectrophotometric method. J Agric Food Chem 49(7): 3133-3139

Garnier E, Laurent G (1994) Leaf anatomy, specific mass and water content in congeneric annual and perennial grass species. New Phytologist 128(4): 725-736

Griffith DM, Quigley KM, Anderson TM (2016) Leaf thickness controls variation in leaf mass per area (LMA) among grazing-adapted grasses in Serengeti. Oecologia 181(4): 1035-1040

Hartikainen SM, Jach A, Grané A, Robson TM (2018) Assessing scale-wise similarity of curves with a thick pen: As illustrated through comparisons of spectral irradiance. Joural Ecology and Evolution 8(20): 10206-10218

Hayes S, Velanis CN, Jenkins GI, Franklin KA (2014) UV-B detected by the UVR8 photoreceptor antagonizes auxin signaling and plant shade avoidance. Proc Natl Acad Sci U S A 111(32): 11894-11899

He P, Wright IJ, Zhu S, Onoda Y, Liu H, Li R, Liu X, Hua L, Oyanoghafo OO, Ye Q (2019) Leaf mechanical strength and photosynthetic capacity vary independently across 57 subtropical forest species with contrasting light requirements. New Phytologist 223(2): 607-618

Hikosaka K, Terashima I, Katoh S (1994) Effects of leaf age, nitrogen nutrition and photon flux density on the distribution of nitrogen among leaves of a vine (*Ipomoea tricolor* Cav.) grown horizontally to avoid mutual shading of leaves. Oecologia, 97: 451-457

Hikosaka K, Onoda Y, Kinugasa T, Nagashima H, Anten NPR, Hirose T (2005) Plant responses to elevated CO2 concentration at different scales: leaf, whole plant, canopy, and population. Ecol Res 20(3): 243-253

Hogewoning SW, Trouwborst G, Maljaars H, Poorter H, van Ieperen W, Harbinson J (2010) Blue light dose-responses of leaf photosynthesis, morphology, and chemical composition of Cucumis sativus grown under different combinations of red and blue light. J Exp Bot 61(11): 3107-3117

Hothorn T, Bretz F, Westfall P (2008) Simultaneous inference in general parametric models. Biom J 50(3): 346-363

Hu J, Dai X, Sun G (2016) Morphological and physiological responses of morus alba seedlings under different light qualities. Notulae Botanicae Horti Agrobotanici Cluj-Napoca 44(2): 382-392, Article

Iiyama K, Wallis AF (1990) Determination of lignin in herbaceous plants by an improved acetyl bromide procedure. J Sci Food Agric 51(2): 145-161

Ishizaki S, Hikosaka K, Hirose T (2003) Increase in leaf mass per area benefits plant growth at elevated CO2 concentration. Ann Bot 91(7): 905-914

Jenkins GI (2017) Photomorphogenic responses to ultraviolet-B light. Plant, Cell & Environment 40(11): 2544-2557

Jenkins GI, Long JC, Wade HK, Shenton MR, Bibikova TN (2001) UV and blue light signalling: pathways regulating chalcone synthase gene expression in Arabidopsis. New Phytologist 151(1): 121-131

John GP, Scoffoni C, Buckley TN, Villar R, Poorter H, Sack L (2017) The anatomical and compositional basis of leaf mass per area. Ecol Lett 20(4): 412-425

Julkunen-Tiitto R (1985) Phenolic constituents in the leaves of northern willows: methods for the analysis of certain phenolics. J Agric Food Chem 33(2): 213-217

Kitajima K (1994) Relative importance of photosynthetic traits and allocation patterns as correlates of seedling shade tolerance of 13 tropical trees. Oecologia 98(3-4): 419-428

Kitajima K, Poorter L (2010) Tissue-level leaf toughness, but not lamina thickness, predicts sapling leaf lifespan and shade tolerance of tropical tree species. New Phytol 186(3): 708-721

Li Y, Yang DM, Xiang S, Li GY (2013) Different responses in leaf pigments and leaf mass per area to altitude between evergreen and deciduous woody species. Aust J Bot 61(6): 424-435

Lin C (2000) Plant blue-light receptors. Trends Plant Sci 5(8): 337-342

Liu Y, Wang TL, Fang SZ, Zhou MM, Qin J (2018) Responses of Morphology, Gas Exchange, Photochemical Activity of Photosystem II, and Antioxidant Balance in Cyclocarya paliurus to Light Spectra. Frontiers in Plant Science 9

Moss DN (1967) Solar energy in photosynthesis. Solar Energy 11(3-4): 173-179

Niinemets U (1997) Role of foliar nitrogen in light harvesting and shade tolerance of four temperate deciduous woody species. Funct Ecol 11(4): 518-531

Niinemets U (1999) Components of leaf dry mass per area - thickness and density - alter leaf photosynthetic capacity in reverse directions in woody plants. New Phytologist 144(1): 35-47

Niinemets U (2001) Global-scale climatic controls of leaf dry mass per area, density, and thickness in trees and shrubs. Ecology 82(2): 453-469

O'Hara A, Headland LR, Díaz-Ramos LA, Morales LO, Strid Å, Jenkins GI (2019) Regulation of Arabidopsis gene expression by low fluence rate UV-B independently of UVR8 and stress signaling. Photochem Photobiol Sci 18: 1675-1684

Oguchi R, Hikosaka K, Hirose T (2005) Leaf anatomy as a constraint for photosynthetic acclimation: differential responses in leaf anatomy to increasing growth irradiance among three deciduous trees. Plant Cell Environ 28(7): 916-927

Oguchi R, Hiura T, Hikosaka K (2017) The effect of interspecific variation in photosynthetic plasticity on 4-year growth rate and 8-year survival of understorey tree seedlings in response to gap formations in a cool-temperate deciduous forest. Tree Physiol 37(8): 1113-1127

Onoda Y, Schieving F, Anten NPR (2008) Effects of light and nutrient availability on leaf mechanical properties of Plantago major: A conceptual approach. Ann Bot 101(5): 727-736

Onoda Y, Wright IJ, Evans JR, Hikosaka K, Kitajima K, Niinemets Ü, Poorter H, Tosens T, Westoby M (2017) Physiological and structural tradeoffs underlying the leaf economics spectrum. New Phytologist 214(4): 1447-1463

Onoda Y, Westoby M, Adler PB, Choong AM, Clissold FJ, Cornelissen JH, Díaz S, Dominy NJ, Elgart A, Enrico L (2011) Global patterns of leaf mechanical properties. Ecol Lett

14(3): 301-312

Peeters PJ (2002) Correlations between leaf structural traits and the densities of herbivorous insect guilds. Biol J Linn Soc 77(1): 43-65

Pinheiro JC, Bates DM (2000) Linear mixed-effects models: basic concepts and examples. J Mixed-effects models in SS-Plus: 3-56

Poorter H (1994) Construction costs and payback time of biomass: a whole plant perspective. A whole plant perspective on carbon-nitrogen interactions: 111-127

Poorter H, Villar R (1997) Chemical composition of plants: causes and consequences of variation in allocation of C to different plant constituents. Plant Resource Allocation Academic Press, New York: 39-72

Poorter H, Niinemets Ü, Poorter L, Wright IJ, Villar R (2009) Causes and consequences of variation in leaf mass per area (LMA): a meta-analysis. New Phytologist 182(3): 565-588

Poorter H, Niinemets U, Ntagkas N, Siebenkas A, Maenpaa M, Matsubara S, Pons T (2019) A meta-analysis of plant responses to light intensity for 70 traits ranging from molecules to whole plant performance. New Phytol

Rai N, Neugart S, Yan Y, Wang F, Siipola SM, Lindfors AV, Winkler JB, Albert A, Brosché M, Lehto T (2019) How do cryptochromes and UVR8 interact in natural and simulated sunlight? J Exp Bot erz236

Razzak A, Ranade SS, Strand A, Garcia-Gil MR (2017) Differential response of Scots pine seedlings to variable intensity and ratio of red and far-red light. Plant Cell Environ 40(8): 1332-1340

Reich PB, Walters MB, Ellsworth DS (1997) From tropics to tundra: Global convergence in plant functioning. Proc Natl Acad Sci U S A 94(25): 13730-11373

Rizzini L, Favory JJ, Cloix C, Faggionato D, O'Hara A, Kaiserli E, Baumeister R, Schäfer E, Nagy F, Jenkins GI (2011) Perception of UV-B by the Arabidopsis UVR8 protein. Science 332(6025): 103

Robson TM, Klem K, Urban O, Jansen MA (2015) Re-interpreting plant morphological responses to UV-B radiation. Plant, Cell and Environment 38(5): 856 -866

Robson TM, Aphalo PJ, Banas AK, Barnes PW, Brelsford CC, Jenkins GI, Kotilainen TK,

Labuz J, Martinez-Abaigar J, Morales LO, Neugart S, Pieriste M, Rai N, Vandenbussche F, Jansen MAK (2019) A perspective on ecologically relevant plant-UV research and its practical application. Photochem Photobiol Sci

Rousseaux MC, Julkunen-Tiitto R, Searles PS, Scopel AL, Aphalo PJ, Ballare CL (2004) Solar UV-B radiation affects leaf quality and insect herbivory in the southern beech tree Nothofagus antarctica. Oecologia 138(4): 505-512

Sanchez-Gomez D, Robson TM, Gasco A, Gil-Pelegrin E, Aranda I (2013) Differences in the leaf functional traits of six beech (Fagus sylvatica L.) populations are reflected in their response to water limitation. Environ Exp Bot 87: 110-119

Sancho-Knapik D, Escudero A, Mediavilla S, Scoffoni C, Zailaa J, Cavender-Bares J, Gomez Alvarez-Arenas T, Molins A, Alonso-Forn D, Ferrio JP, Peguero-Pina JJ, Gil-Pelegrin E (2020) Deciduous and evergreen oaks show contrasting adaptive responses in leaf mass per area across environments. The New phytologist

Searles PS, Flint SD, Caldwell MM (2001) A meta analysis of plant field studies simulating stratospheric ozone depletion. Oecologia 127(1): 1-10

Smith H (2000) Phytochromes and light signal perception by plants - an emerging synthesis. Nature 407(6804): 585-591

Smith HL, McAusland L, Murchie EH (2017) Don't ignore the green light: exploring diverse roles in plant processes. J Exp Bot 68(9): 2099-2110

Terashima I, Fujita T, Inoue T, Chow WS, Oguchi R (2009) Green light drives leaf photosynthesis more efficiently than red light in strong white light: revisiting the enigmatic question of why leaves are green. Plant Cell Physiol 50(4): 684-697, Review

Terfa MT, Solhaug KA, Gislerød HR, Olsen JE, Torre S (2013) A high proportion of blue light increases the photosynthesis capacity and leaf formation rate of Rosa × hybrida but does not affect time to flower opening. Physiol Plant 148(1): 146-159

Valladares F, Niinemets U (2008) Shade Tolerance, a Key Plant Feature of Complex Nature and Consequences. In: Annual Review of Ecology Evolution and Systematics. pp 237-257

Verdaguer D, Jansen MA, Llorens L, Morales LO, Neugart S (2017) UV-A radiation effects on higher plants: Exploring the known unknown. Plant Sci 255: 72-81

Wang Q-W, Daumal M, Nagano S, Yoshida N, Morinaga S-I, Hikosaka K (2019) Plasticity of functional traits and optimality of biomass allocation in elevational ecotypes of Arabidopsis halleri grown at different soil nutrient availabilities. J Plant Res 132(2): 237-249

Wang Q-W, Liu C-G, Zhou W, Qi L, Zhou L, Yu D, Dai L (2018a) Mobile carbon supply in trees and shrubs at the alpine treeline ecotone. Plant Ecol 219(4): 467-479

Wang Q-W, Robson TM, Pieristè M, Oguro M, Oguchi R, Murai Y, Kurokawa H (2020) Testing trait plasticity over the range of spectral composition of sunlight in forb species differing in shade tolerance. J Ecol 108(5): 1923–1940

Wang QW, Qi L, Zhou W, Liu CG, Yu D, Dai L (2018b) Carbon dynamics in the deciduous broadleaf tree Erman's birch (*Betula ermanii*) at the subalpine treeline on Changbai Mountain, Northeast China. Am J Bot 105(1): 42-49

Waterman PG, Mole S (1994) Analysis of phenolic plant metabolites. Blackwell Scientific,

Wilson PJ, Thompson K, Hodgson JG (1999) Specific leaf area and leaf dry matter content as alternative predictors of plant strategies. New phytologist 143(1): 155-162

Witkowski E, Lamont BB (1991a) Leaf specific mass confounds leaf density and thickness. Oecologia 88(4): 486-493

Witkowski ET, Lamont BB (1991b) Leaf specific mass confounds leaf density and thickness. Oecologia 88(4): 486-493

Wright IJ, Westoby M, Reich PB (2002) Convergence towards higher leaf mass per area in dry and nutrient-poor habitats has different consequences for leaf life span. J Ecol 90(3): 534-543

Wright IJ, Reich PB, Westoby M, Ackerly DD, Baruch Z, Bongers F, Cavender-Bares J, Chapin T, Cornelissen JHC, Diemer M, Flexas J, Garnier E, Groom PK, Gulias J, Hikosaka K, Lamont BB, Lee T, Lee W, Lusk C, Midgley JJ, Navas ML, Niinemets U, Oleksyn J, Osada N, Poorter H, Poot P, Prior L, Pyankov VI, Roumet C, Thomas SC, Tjoelker MG, Veneklaas EJ, Villar R (2004) The worldwide leaf economics spectrum. Nature 428(6985): 821-827

Xu CY, Salih A, Ghannoum O, Tissue DT (2012) Leaf structural characteristics are less important than leaf chemical properties in determining the response of leaf mass per

area and photosynthesis of Eucalyptus saligna to industrial-age changes in CO2 and temperature. J Exp Bot 63(16): 5829-5841

Yeo IK, Johnson RA (2000) A new family of power transformations to improve normality or symmetry. Biometrika 87(4): 954-959

Zhang L, Yang L, Shen W (2020) Dramatic altitudinal variations in leaf mass per area of two plant growth forms at extreme heights. Ecological Indicators 110

Zhang T, Maruhnich SA, Folta KM (2011) Green light induces shade avoidance symptoms. Plant Physiology 157(3): 1528-1536

Zhang X, Jin G, Liu Z (2019) Contribution of leaf anatomical traits to leaf mass per area among canopy layers for five coexisting broadleaf species across shade tolerances at a regional scale. Forest Ecology and Management 452 (15), 117569

Supporting information

Table S1 Correlations among leaf morphological and biochemical traits on a dry-matter basis.

Table S2 Correlations among leaf morphological and biochemical traits on an area basis.

Fig. S1 Photographs of the spectral-attenuation experiment in the common garden.

Fig. S2 Daily solar irradiance and temperature during the period of the common garden experiment.

Fig. S3 Variation in leaf mass and leaf area under spectral irradiance treatments.

Fig. S4 Variation in leaf chemical composition: dry-matter concentrations under spectral irradiance treatments.

Fig. S5 Variation in leaf chemical composition: concentrations given on an area basis under spectral irradiance treatments.

Figure ledends

Fig. 1 Variation in (A) leaf mass per area (LMA), (B) leaf density (LD), and (C) leaf thickness (LT) under different spectral irradiance treatments. Each point represents the mean ± 1 SE trait value of the individuals of each treatment. n=9-11 replicates (one replicate being one plant with 1 measure per plant). Data was analysed using linear mixed effect models (LME), including treatments as fixed factors, and species and blocks as random factors. Treatment effect is shown by $\chi^2$and *P* values. The specific effect of each spectral region is given by contrast comparison between pairs of treatments. * indicates statistically significant difference ($P < 0.05$) and ns represents no significant difference ($P > 0.05$), tested by Benjamini-Hochberg (BH)'s method.

Fig.2 Relationship between (A) leaf mass per area (LMA) with leaf density (LD), (B) LMA with leaf thickness (LT), and between (C) LT with LD across species for each spectral treatment. LMA and LD values were transformed by the Box–Cox power transformation. Solid coloured lines denote significant relationships ($P < 0.05$), tested by Linear least squares method. R^2 values of the significant relationships were shown next to the respective legend markers. Detailed statistical analyses coefficient and *P* values are in Table S1.

Fig.3 Relationship between (A) leaf mass per area (LMA), (B) leaf density (LD), and (C) LMA with leaf chemical concentrations across species for each spectral treatment. Values of LMA, LD, phenolics, tannins, sugars, starch, and non-structure carbohydrates (NSC) were transformed by the Box–Cox power transformation. Solid coloured lines denote significant relationships ($P < 0.05$), tested by Linear least squares method. Detailed coefficient and *P* values are in Table 3. C, carbon; N, nitrogen.

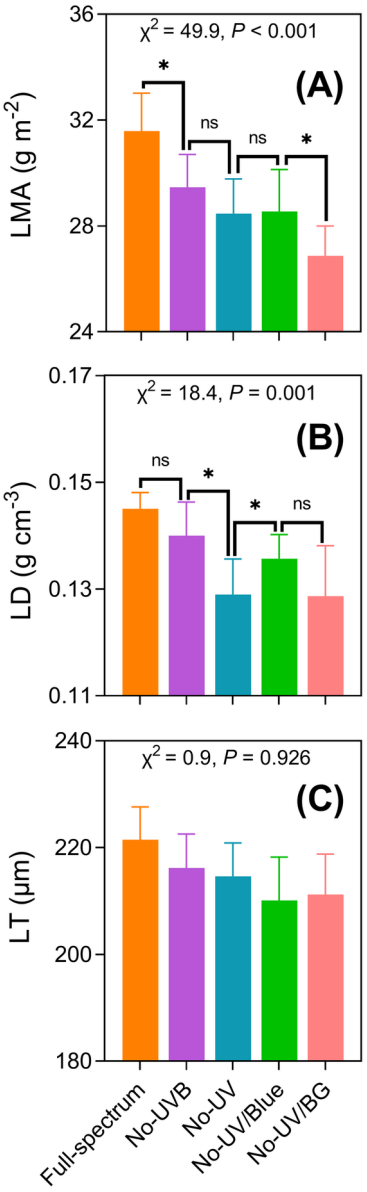

PPL_13512_Figure1.tif

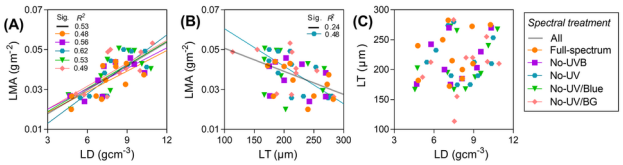

PPL_13512_Figure2.tif

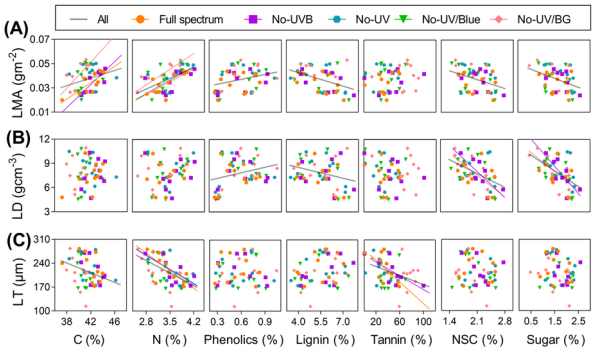

PPL_13512_Figure3.tif

Table 1 List of plant species and leaf traits in the common garden experiment and their functional classification. Leaf traits of each species were measured from the Full-spectral treatment (ambient sunlight group) at the end of the common garden experiment. Mean values (SE) are shown for each species (n=11 replicates with one replicate being one plant and 1 measure per plant). LMA, leaf mass per area; LM, leaf mass; LA, leaf area; LT, leaf thickness; LD, leaf density; C, carbon; N, nitrogen; NSC, non-structural carbohydrates.

Traits	*Adenophora triphylla var. japonica*	*Artemisia indica var. maximowiczii*	*Eupatorium japonicum*	*Eupatorium makinoi*	*Fallopia japonica*	*Geum aleppicum*	*Geum japonicum*	*Plantago asiatica*	*Platycodon grandiflorus*	*Prunella vulgaris subsp. asiatica*	*Senecio cannabifolius*
LMA (g m^{-2})	30.6(0.42)	22.7(0.77)	23.8(1.16)	37.3(1.22)	26.7(1.82)	23.2(1.18)	37.5(0.37)	49.8(3.70)	39.7(0.75)	24.0(1.29)	28.8(1.45)
LM (g)	0.15(0.016)	0.03(0.002)	0.10(0.003)	0.24(0.071)	0.06(0.003)	0.06(0.005)	0.30(0.002)	0.09(0.013)	0.19(0.035)	0.03(0.001)	0.04(0.005)
LA (cm^2)	47.4(4.82)	14.9(0.69)	42.0(2.21)	64.0(16.97)	21.4(2.71)	24.6(3.05)	79.3(0.49)	18.2(3.16)	48.1(9.12)	12.8(0.75)	12.8(1.56)
LT (um)	272(4.79)	185(6.45)	172(14.4)	250(20.0)	275(25.0)	210(15.8)	182(8.00)	240(14.1)	283(9.46)	200(18.7)	215(16.6)
LD (g cm^{-3})	0.11(0.001)	0.12(0.003)	0.14(0.006)	0.15(0.007)	0.10(0.002)	0.11(0.011)	0.21(0.008)	0.21(0.02)	0.14(0.006)	0.12(0.01)	0.14(0.010)
C (%)	42.9(0.46)	43.5(0.18)	42.6(0.45)	41.3(2.25)	41.1(0.85)	44.0(0.29)	42.2(0.73)	37.2(2.33)	40.1(0.98)	42.6(0.14)	43.2(0.27)
N (%)	3.18(0.19)	3.91(0.06)	3.91(0.14)	3.19(0.08)	3.00(0.22)	3.99(0.09)	3.08(0.27)	3.38(0.13)	2.83(0.16)	3.61(0.03)	3.46(0.20)
Phenolics (%)	4.76(0.30)	5.51(0.44)	1.63(0.12)	2.29(0.47)	8.31(0.16)	2.53(0.43)	13.9(1.30)	10.53(1.05)	2.46(0.26)	3.77(0.22)	1.45(0.08)
Lignin (%)	6.63(0.14)	5.62(0.12)	4.39(0.15)	5.31(0.64)	5.10(0.30)	4.01(0.05)	6.51(0.14)	7.04(0.12)	5.88(0.09)	6.05(0.18)	3.93(0.15)
Tannin (%)	0.94(0.29)	0.13(0.014)	0.13(0.02)	0.19(0.03)	0.19(0.03)	0.15(0.02)	0.18(0.01)	0.16(0.03)	0.17(0.01)	0.20(0.03)	0.16(0.01)
NSCs (%)	6.16(0.26)	12.0(0.44)	5.76(0.49)	6.61(0.38)	9.24(0.66)	5.89(0.37)	10.9(0.35)	12.17(0.59)	7.29(0.48)	5.13(0.15)	12.9(1.07)
Sugars (%)	3.11(0.35)	9.26(0.41)	4.12(0.61)	4.29(0.41)	5.18(0.26)	3.34(0.32)	7.99(0.39)	8.35(0.87)	4.18(0.21)	2.42(0.11)	7.26(1.27)
Starch (%)	3.06(0.36)	2.72(0.24)	1.65(0.12)	2.32(0.28)	4.06(0.40)	2.54(0.44)	2.92(0.22)	3.81(0.71)	3.11(0.41)	2.71(0.18)	5.60(0.56)

Table 2 Transmittance, spectral photon irradiances, and temperature under filters with shade meshes in the growth experiment. Values indicate means (n=4).

Filters	Quantity	Transmittance (%)							Photon irradiances (µmol m^{-2} s^{-1})							Temp (°C)
		PAR	UV-B	UV-A	Blue	Green	Red	Far-red	PAR	UV-B	UV-A	Blue	Green	Red	Far-red	
Polythene	>280 nm	14.0	10.1	12.5	13.5	13.9	14.3	14.8	231.5	0.4	17.6	45.8	56.6	52.3	39.8	29.1
Polyester	>315 nm	13.4	0.0	8.8	12.8	13.4	13.8	14.3	302.2	0.0	16.2	58.6	74.2	69.2	52.5	29.6
Rosco 226	>400 nm	13.6	0.2	1.3	13.1	13.8	14.2	14.4	261.0	0.0	2.0	50.7	64.6	60.2	45.3	29.5
Rosco 312	>500 nm	14.9	0.1	0.7	0.9	17.0	22.1	22.9	287.6	0.0	1.1	3.5	80.0	94.4	72.6	29.3
Rosco 135	>580 nm	12.5	0.0	0.3	0.3	0.8	29.4	32.1	238.9	0.0	0.4	1.1	3.7	125.3	101.1	29.2

Note: Filters were combined with different shade meshes to make light intensity similarly under all frames in the experiment. Measurements were done by A Maya 2000 Pro (Ocean Optics) spectrometer under each of the filters of 23-07-2018 at midday under a clear sky. Immediately after (within 2 minutes) each filter measurement, they were compared with the ambient solar spectral irradiance measured adjacent to the filter. Wavelength ranges in nm, PAR: 400–700; UV-B: 280–315; UV-A: 315–400; Blue: 420–490; Green: 500–580; Red: 580–700; Far-red: 710–850. The temperature was recorded at 30-min intervals using a HOBO H8 Pro temperature logger (Onset Computer Corporation).